Electrochemistry and time dependent DFT study of a (vinylenedithio)-TTF derivative in different oxidation states

Halpin, Yvonne; Schulz, Martin; Brooks, Andrew C.; Browne, Wesley R.; Wallis, John D.; Gonzalez, Leticia; Day, Peter; Vos, Johannes G.

Published in:
Electrochimica Acta

DOI:
10.1016/j.electacta.2013.03.114

Publication date:
2013

Electrochimica Acta 100 (2013) 188–196

Contents lists available at SciVerse ScienceDirect

Electrochimica Acta

journal homepage: www.elsevier.com/locate/electacta

Electrochemistry and time dependent DFT study of a (vinylenedithio)-TTF derivative in different oxidation states

Yvonne Halpin[a], Martin Schulz[b], Andrew C. Brooks[c,f], Wesley R. Browne[d], John D. Wallis[c,**], Leticia González[e], Peter Day[f], Johannes G. Vos[a,*]

[a] Solar Energy Conversion SRC, School of Chemical Sciences, Dublin City University, Dublin 9, Ireland
[b] Pharmaceutical Radiochemistry, Technical University, Munich, Walther-Meißner Str 3, 85748 Garching, Germany
[c] School of Science and Technology, Nottingham Trent University, Clifton Lane, Nottingham NG11 8NS, United Kingdom
[d] Center for Systems Chemistry, Stratingh Institute for Chemistry and Zernike Institute for Advanced Materials, Faculty of Mathematics and Natural Sciences, University of Groningen, Nijenborgh 4, 9747AG Groningen, The Netherlands
[e] Institute for Theoretical Chemistry, University Vienna, Währinger Str. 17, A-1090 Vienna, Austria
[f] University College London, Department of Chemistry, 20 Gordon Street, London WC1H 0AJ, United Kingdom

ARTICLE INFO

Article history:
Received 22 January 2013
Received in revised form 16 March 2013
Accepted 16 March 2013
Available online xxx

Keywords:
Tetrathiafulvalene
Pyridine
Monolayer
Density functional theory

ABSTRACT

The electrochemical and spectroelectrochemical properties of a bis-pyrid-4-yl functionalised vinylenedithio-TTF derivative, **1**, in solution are reported. The compound was immobilised on a Pt electrode and the resulting layers formed were investigated using electrochemical techniques. Two oxidation processes were observed for **1**, typical of TTF derivatives. A solvent dependence study revealed that the stabilisation of the radical cation intermediate, $\mathbf{1}^{\bullet+}$, towards further oxidation is achieved in solvents with a low Gutmann donor number such as dichloromethane. Analysis of $\mathbf{1}^{2+}$ in solution under aerobic and anaerobic conditions reveal that its stability is compromised in the presence of oxygen and therefore the stability of monolayers of **1** is greatly enhanced under anaerobic conditions. Time dependent DFT calculations of the compound in several oxidation states are discussed to obtain information on the location of the various redox processes.

1. Introduction

In the latter half of the 20th century the discovery of metal-like behaviour in the organic compound, tetrathiafulvalene (TTF) [1] has led to considerable interest in TTF derivatives. Extensive studies have been performed on properties such as metal-like conductivity and superconductivity of organic salts and charge transfer complexes incorporating the TTF core [2–4]. The strong π-electron donor properties of the TTF unit have attracted significant attention in the development of donor-acceptor systems exhibiting both intermolecular (TTF-TCNQ [5]) and intramolecular charge transfer properties [6–8]. Adding to this, TTF complexes are also useful building blocks for supramolecular systems [9–13]. There are several advantages associated with using the redox active TTF core as a building block for more advanced materials: upon oxidation of the TTF ring system, a thermodynamically stable cation radical is formed and further oxidation results in formation of the dication; both of these processes are electrochemically quasi-reversible and occur within a readily accessible potential window. By adding electron donating/withdrawing groups to the TTF core, the oxidation potentials can be tuned [2]. The non-aromatic 14 π-electron system undergoes aromatisation when going from the neutral species to the dithiolium form in the singly and doubly oxidised states. TTF and its derivatives have featured in a wide variety of applications from crown-ether annelated electrochemical sensors [13–16], to molecular electronics [17–21] including organic field-effect transistors [22] and other advanced molecular assemblies [23–25].

An important feature in the development of such nanostructures is the immobilisation of the associated molecules on a surface creating mono/multilayers and providing a route to organisation within the assembly. This proposed organisation within the monolayer is not only a function of the behaviour of, and interaction between the molecules themselves, but also the interaction between the molecules and the surface [26]. Stable redox chemistry in self-assembled monolayers of TTF derivatives have been reported by several groups including those of Bryce, Ward, Cooke, Sallé, Echegoyen and Stoddart, where the core TTF moiety is anchored to the surface using a surface active functional group such as an alkyl chain with a thiol end group on Au [13,14,27–30], thioctic acid disulfide linkers on Au [31–33] and oxide-free

* Corresponding author. Tel.: +353 1 700 5307; fax: +353 1 700 5503.
** Corresponding author. Tel.: +Tel.: +44 115 848 8053; fax: +44 115 848 8077.
E-mail addresses: john.wallis@ntu.ac.uk (J.D. Wallis), han.vos@dcu.ie, hanvos61@gmail.com (J.G. Vos).

0013-4686/$ – see front matter © 2013 Elsevier Ltd. All rights reserved.
http://dx.doi.org/10.1016/j.electacta.2013.03.114

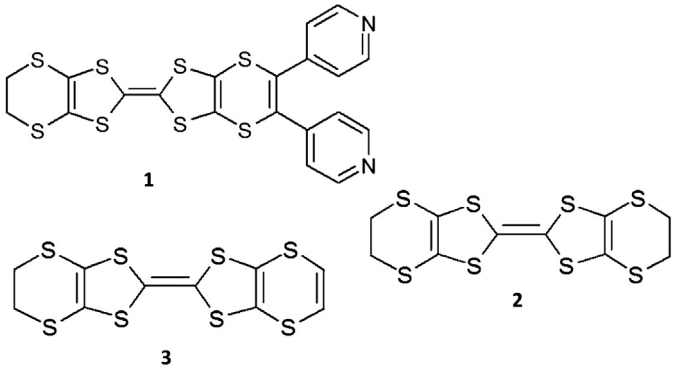

Fig. 1. Molecular structures of TTF derivatives **1**, **2** and **3**.

hydrogen-terminated Si(1 0 0) surfaces [34]. Non-covalent binding of TTF derivatives on graphite has also been reported where the molecule's core TTF unit has a strong interaction with the π-system of the graphite surface; this allows the molecule to orientate parallel to the graphite surface through π–π interactions [35,36]. However, the addition of amide groups on the TTF core results in this unit orientating orthogonally to the graphite surface as opposed to in plane [35].

The presence of long alkyl chains as the surface linkers in a monolayer can be unfavourable when the redox active species is intended for use in highly conducting layers designed for the fabrication of electronic devices [37]. The work presented herein is focused on a bis(pyrid-4-yl) functionalised 4,5-ethylenedithio-4′,5′-vinylenedithiotetrathiafulvalene derivative (EVT-TTF) (**1**) (Fig. 1), in which the substituted carbons are connected by a double bond (the synthesis and characterisation of which has been reported previously) [38]. The nitrogen atom of the pyridine ring has been reported to have a strong affinity for Pt resulting in the formation of stable monolayers [39–41] and in systems which are potentially suitable for use in molecular electronic devices [42–45]. The absence of long alkyl chain linker groups in **1** may be favourable for forming conductive layers on the surface. The electrochemical properties of **1** are presented for both the solution phase and as monolayers formed on platinum. The electronic and electrochemical properties of the compound in different oxidation states are investigated using time-dependent DFT techniques. The results obtained herein are compared with those of bis(ethylenedithio)tetrathiafulvalene, **2** and the unsymmetrical TTF derivative, 4,5-ethylenedithio-4′,5′-vinylenedithiotetrathiafulvalene, **3** [46] (Fig. 1).

2. Experimental

2.1. Electrochemistry

Prior to analysis, the surface of the platinum working electrode was prepared by polishing sequentially using 1.0, 0.3 and 0.05 μm alumina slurry (CH Instruments, Inc.) followed by sonication in deionised water for 5 min after each successive polishing with the alumina slurry. The Pt electrode was then electrochemically cleaned by cycling in 0.5 M H_2SO_4 followed by sonication in the appropriate solvent. Electrochemical experiments were carried out using a CH Instruments Version 8.15 software controlled electrochemical bipotentiostat (CHI750C). Typical concentrations of 1 mM were used for solution phase electrochemical measurements throughout. A Pt wire was used as the counter electrode with either a Ag/AgCl (3 M KCl solution) or a Hg/$HgSO_4$ (saturated K_2SO_4) as the reference electrode. All potentials are referenced against the Saturated Calomel Electrode (SCE) using ferrocene as an internal standard. Cyclic voltammograms were recorded using 0.1 M tetrabutylammonium hexafluorophosphate ($TBAPF_6$, Fluka electrochemical grade ≥99.0%) in dichloromethane (CH_2Cl_2, Aldrich anhydrous, 99.8%) as the electrolyte. Where anaerobic environments were required, prior to experiments, the solutions were deoxygenated with argon and a blanket of argon was maintained during analysis. The solvent dependence was investigated using $TBAPF_6$ as electrolyte in dimethylformamide (DMF, Aldrich spectrophotometric grade, 99.8%), acetone (Aldrich, spectrophotometric grade, ≥99.5%) and tetrahydrofuran (THF, Aldrich, HPLC grade 99.9%). As well as $TBAPF_6$, both tetrabutylammonium perchlorate ($TBAClO_4$, Fluka electrochemical grade, ≥99.0%) and potassium hexafluorophosphate (KPF_6, Aldrich, 99.99%) were used with CH_2Cl_2 and acetone to investigate the influence of the electrolyte on the redox properties.

2.2. Monolayer formation

Monolayers of **1** were formed on a Pt substrate using a solution phase deposition method. The Pt electrode was first pre-treated using the polishing and electrochemical cleaning method described above. The clean metal electrode was then immersed in a 500 μM solution of **1** in CH_2Cl_2 for 24 h. Prior to the experiment the electrode was removed from the deposition solution and rinsed with acetonitrile (Aldrich anhydrous, 99.8%) to ensure the removal of any unbound material. Either 0.1 M tetrabutylammonium tetrafluoroborate ($TBABF_4$, Fluka electrochemical grade ≥99.0%) or $TBAClO_4$ in acetonitrile were used as electrolyte.

2.3. Oxidative spectroelectrochemistry

JASCO 630 UV–vis and 570 UV–vis-NIR spectrophotometers were used to record the UV–vis-NIR absorption data. The potentials were controlled using bulk electrolysis on a model CHI760C bipotentiostat (CH Instruments, Inc.). Analyte concentrations were typically 0.5–1.0 mM. CH_2Cl_2 and $TBAPF_6$ were used as solvent and electrolyte with a Ag wire as reference electrode. A Pt wire and Pt gauze were used as the counter and working electrodes respectively. Preparation of the Pt gauze electrode comprised of electrochemical cycling in 0.5 M H_2SO_4. A custom made 2 mm path length quartz cuvette (volume: 1.2 mL) was employed for all oxidative spectroelectrochemical measurements. The absorbance maxima are ±1 nm.

2.4. Modelling of electronic properties

Geometry was optimised with the GAUSSIAN 03 programme [47] in the gas phase at the B3PW91/6-31+G(d) [48–52] level of theory without constraints to symmetry. The default Berny optimisation algorithm and the default threshold values for the maximum force and displacement were used for **1** and **2** and GDIIS to optimise $\mathbf{1}^{\bullet+}$ and $^{1}\mathbf{1}^{2+}$ [53–55]. Stationary points were confirmed as local minima by a frequency calculation (absence of imaginary frequencies). The charged species were calculated with unrestricted wave functions. Single point energy calculations and time-dependent DFT (TD-DFT) [56–58] were performed with the Gaussian 03 programme at the B3PW91/6-31+G(d) level and the Gaussian 09 programme [59] at the BMK [60]/6-31+G(d), M06HF [61]/6-31+G(d) and BMK/def2-TZVPP+R [62,63] level of theory employing the CPCM [64,65] solvent model and dichloromethane as the solvent [66]. Full convergence of the SCF procedure was requested with the *SCF = tight* keyword. Atomic radii were calculated by the Universal Force Field (UFF) method, which is the default in Gaussian 09. Percent contributions and density of states (DOS) of selected groups were analysed with the GaussSum programme

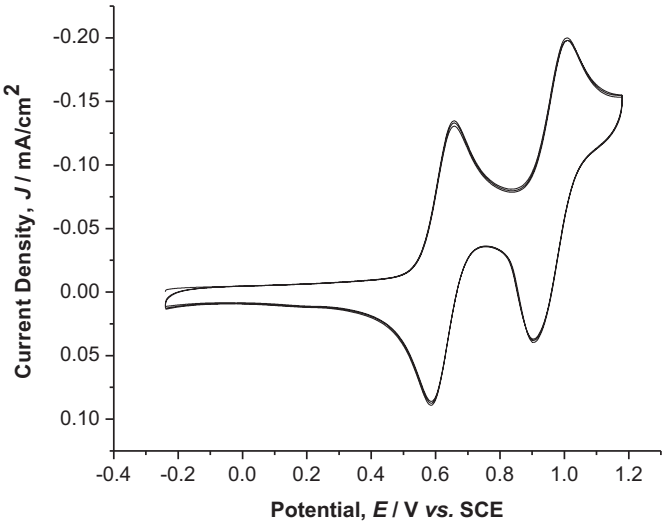

Fig. 2. Cyclic voltammogram of **1** [C: 1 mM], at a platinum working electrode, in CH_2Cl_2 with 0.1 M $TBAPF_6$. Scan rate: 100 mV/s.

[67] based on a Mulliken population analysis. Absorption spectra were calculated with 40 states.

3. Results and discussion

3.1. Electrochemistry

The oxidative electrochemistry of **1** is shown in Fig. 2. The resulting electrochemical parameters obtained in a range of solvents are shown in Table 1.

The two reversible redox waves observed in the cyclic-voltammogram (CV) for **1** are characteristic of the oxidative electrochemistry of TTF and its derivatives [2–4]. The first process corresponds to the oxidation of the neutral species forming the monocation radical, $\mathbf{1}^{\bullet+}$ at +0.62 V, *vs.* SCE, with a peak-to-peak separation, ΔE_p, of 70 mV (see Fig. 2). At higher potentials the formation of the dication $\mathbf{1}^{2+}$ is observed (+0.95 V, *vs.* SCE, ΔE_p = 100 mV). DFT calculations discussed below confirm that the oxidations are centred on the TTF core and not on the pyridyl rings. Comparison of the oxidative electrochemistry, recorded for compounds **1**, **2** [68] and **3** [46] with that reported for TTF [69] further confirms this assignment and indicates that the oxidation potentials and therefore HOMO levels, are sensitive to the electron donating/withdrawing properties of substituents on the dithiole rings, this is confirmed by the DFT calculations shown below.

The electron withdrawing ethylenedithio groups of **2** stabilise the HOMO levels and increase the oxidation potentials (in CH_2Cl_2) by 200 mV compared to TTF. In compound **3**, the first redox process occurs (in THF) at a potential that is 60 mV more positive than observed in **2** as a result of the addition of a double bond in the dithiin ring [46]. A similar increase in the oxidation potential of the first redox process in **1** compared to **2** is observed (Table 1). As a result of the additional electron withdrawing properties of the pyridine rings in **1**, a further increase in the oxidation potential of the first anodic process relative to the un-substituted **3** may be expected. These values are similar to those observed for other related pyridine substituted TTF compounds [70].

Reductive solution phase cyclic voltammetry of **1** (within a potential window of 0 to −2.0 V) reveals two irreversible processes (E_{pc} = −1.41 and −1.80 V, *vs.* SCE). TTF compounds have an electron rich core and exhibit strong π-donor properties. There are relatively few reports of reduction potentials of the TTF component in such systems. Reduction potentials have been reported by Shen and co-workers [71] for perylene substituted TTF derivatives and by Martín and co-workers [72] for benzoquinone substituted TTF dyads. In both cases reduction of the compound was assigned to being based on the perylene and benzoquinone moieties and not the TTF core itself. As outlined below, DFT studies carried out for **1** reveal a LUMO that is comprised of collective contributions of over 50% from the pyridine rings whereas the TTF core itself contributes 4%, *vide infra*. It is, therefore, reasonable to suggest that the cathodic processes observed for **1** are taking place at the pyridine rings and not the central TTF moiety [73].

3.2. Solvent dependence

The influence of the solvent and electrolyte on the oxidative electrochemical properties of **1** was investigated and the effects of solvent parameters such as Lewis basicity/acidity (Gutmann donor/acceptor numbers [74]), polarity [75] and dielectric constant [76] were considered. Table 1 shows that the potential of the first redox process is largely solvent independent, however, the separation ΔE (mV) between the first and second redox waves is sensitive to changes in the solvent-electrolyte medium. As Table 1 indicates, the most important solvent parameter in this case is the donor number (DN). Importantly, upon an increase of this parameter from CH_2Cl_2 to DMF, the separation between the two waves decreases, *i.e.* they are inversely proportional to one another (R^2 = 0.98).

This observation indicates that for the radical monocation intermediate $\mathbf{1}^{\bullet+}$, the positive charge of the radical cation is stabilised by solvation by a nucleophilic solvent. As a result, oxidation of the monocation radical $\mathbf{1}^{\bullet+}$ to $\mathbf{1}^{2+}$ becomes thermodynamically easier [77]. For this reason the spectroelectrochemical experiments carried out in this study were carried out in CH_2Cl_2, the solvent that presents the largest separation between the two redox processes.

3.3. Influence of supporting electrolyte

The effect of electrolyte on the redox properties of species in solution through ion-pairing has been reported for other organic and inorganic systems [78–80]. The influence of anion-pairing on the redox chemistry of **1** was examined through the use of $TBAPF_6$ and $TBAClO_4$ as electrolyte (Table 2).

From the ΔE values recorded for both electrolytes in CH_2Cl_2 it is clear that the degree of separation between the first and second redox wave is heavily dependent on the nature of the anion component of the electrolyte. With ClO_4^- the value of ΔE is 240 mV

Table 1
Electrochemical data for **1** in various solvents under anaerobic conditions, recorded at a Pt macro working electrode. All potentials are quoted *vs.* the SCE. AN and DN are the Gutmann acceptor and donor numbers, respectively. Electrochemical data for **TTF** and reference compounds **2** and **3** included below.

Solvent	$E_{½}$ (V) (ΔE_p (mV))	$E_{½}$ (V) (ΔE_p (mV))	ΔE (mV)	AN	DN	Polarity index[40]	Dielectric constant (ε)[41]
CH_2Cl_2	+0.62 (70)	+0.95 (100)	330	20.4	0	3.1	8.9
Acetone	+0.64 (70)	+0.81 (75)	170	12.5	17	5.1	21.0
THF	+0.73 (90)	+0.83 (65)	100	8	20	4.0	7.5
DMF	+0.66 (60)	+0.75 (50)	90	16	26.6	6.4	38.3

TTF: $E_{½}$ = +0.30, +0.67 V (CH_2Cl_2, *vs.* SCE) [34], **2**: $E_{½}$ = +0.52, +0.94 V (CH_2Cl_2, *vs.* SCE) [33,68], +0.69 V (THF, *vs* SCE)[46] **3**: $E_{½}$ = +0.75 V (THF, *vs.* SCE) [46].

Table 2
Electrochemical data for **1** detailing the changes observed with different electrolytes. All potentials are quoted *vs.* the SCE reference electrode.

Electrolyte	$E_{½}$ (V) (ΔE_p (mV)	$E_{½}$ (V) (ΔE_p (mV)	ΔE (mV)
$TBAPF_6$ in CH_2Cl_2	+0.62 (70)	+0.95 (100)	330
$TBAClO_4$ in CH_2Cl_2	+0.66 (70)	+0.90 (100)	240
$TBAPF_6$ in acetone	+0.64 (60)	+0.81 (65)	170
KPF_6 in acetone	+0.55 (90)	+0.72 (75)	170

Table 3
UV–vis absorption spectroscopic data for compounds **1** (in dichloromethane), **2** and **3** and their different oxidation states and the parent TTF.

Compound	Absorption λ_{max}/nm
1	252, 316, 346, 450 (weak)
$\mathbf{1}^{\bullet+}$	424, 457, 479, 561, 924
$\mathbf{1}^{2+}$	280, 290, 342, 453, 477, 560, 909
2[a]	324, 349, 466 [81]
$\mathbf{2}^{\bullet+}$[a]	458, 486, 599, 992 [81]
3[b]	318, 344 [46]
TTF[c]	303, 317, 368, 450 [82]
$TTF^{\bullet+}$[d]	400, 433, 492, 580 [83]
TTF^{2+}[d]	273, 353 [84]

[a] Recorded in 1,1,2-trichloroethane.
[b] Recorded in tetrahydrofuran.
[c] Recorded in cyclohexane.
[d] Recorded in acetonitrile.[81.]

compared to 330 mV with PF_6^-. This suggests that ClO_4^- provides for tighter ion pairing with oxidation to $\mathbf{1}^{2+}$ at less positive potentials than that observed with PF_6^- [78]. The influence of the cationic component of the electrolyte indicates that the observed effect on ΔE is confined to anions as the ΔE values obtained for $TBAPF_6$ and KPF_6 in acetone are the same, as shown in Table 2.

3.4. Oxidative spectroelectrochemistry

Spectroelectrochemical studies were carried out to obtain information about the electronic properties of the radical monocation, $\mathbf{1}^{\bullet+}$. As outlined below, measurements were carried out in CH_2Cl_2 to investigate the stability of this species. Fig. 3 shows the changes in the UV–vis-NIR absorption spectrum upon oxidation of **1** to $\mathbf{1}^{\bullet+}$ *via* bulk electrolysis at +0.7 V (*vs.* Ag wire). Table 3 lists the UV–vis absorption spectroscopic data for **1** and its oxidised forms and these values are compared with those reported for **2** [81], **3** [46] and the parent TTF compound [82–84]. Four absorbance bands are observed in the spectrum of **1** prior to oxidation. Comparing these values with those reported for **2** and **3** it is noted that there are two common features in the spectra of all three compounds. The two lower energy transitions reported for **2** are in good agreement with those reported for TTF with the bands at 466 and 349 nm. The DFT results indicate that these represent the transitions from the HOMO (π) to the LUMO (σ^*) and from the HOMO to LUMO + 1 $\pi \rightarrow \pi^*$ respectively. Andreu et al. [81] proposed that the absorbance band at 324 nm is composed of three energetically similar bands. The absorbance bands of **1** at 316, 346 and ~450 nm are close in energy to those observed in the absorbance spectrum of **2** (324, 349 and 466 nm) and **3** (318 and 344 nm). Considering this, it may be proposed that these bands represent similar transitions in **1**. This issue is further addressed in the DFT section below.

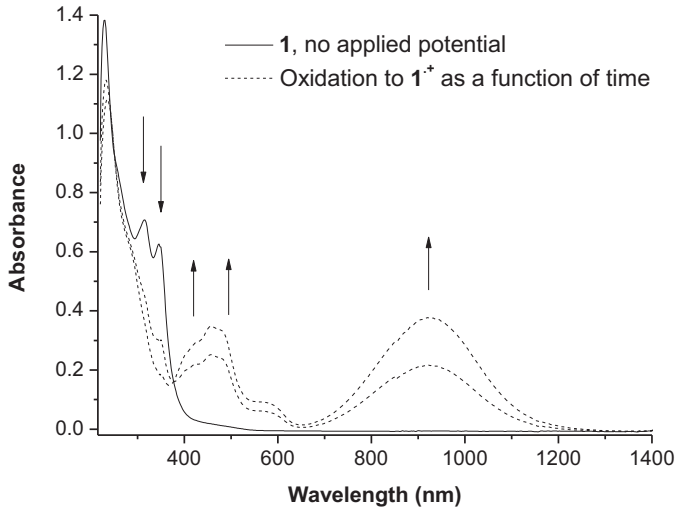

Fig. 3. Spectral changes for **1** (solid black line) with controlled electrochemical oxidation (E = +0.7 V, *vs.* Ag wire) to $\mathbf{1}^{\bullet+}$ as a function of time (dashed black lines). Recorded in CH_2Cl_2 (0.1 M $TBAPF_6$) in air at a Pt gauze working electrode.

For $\mathbf{1}^{\bullet+}$ a decrease in the absorbance bands at 316 and 346 nm is observed with the appearance and concomitant increase in new absorbance bands at 424, 457, 479, 561 and 924 nm (see Fig. 3). There are similarities between the energies of the absorption bands of $\mathbf{1}^{\bullet+}$ and those of $\mathbf{2}^{\bullet+}$ (Table 3) with the lowest energy absorbance band at 992 nm assigned by DFT as the transition of charge from the HDOMO (highest doubly occupied molecular orbital) to the SOMO created upon oxidation to $\mathbf{2}^{\bullet+}$ [81].

An isosbestic point is observed in the absorption spectra at 376 nm (Fig. 3) indicating that conversion from **1** to $\mathbf{1}^{\bullet+}$ is a direct reaction with no intermediates or side products formed. The electrochemical ΔE_p value of 70 mV indicates that this process is reversible. The resulting absorption spectrum from reduction of $\mathbf{1}^{\bullet+}$ back to **1** supports this with almost complete reversibility observed on the timescale of the experiment and shows that the monocation radical species is stable in air.

With continuous cycling between 0 and +1.2 V (*vs.* Ag/AgCl) in aerobic conditions, the dication shows limited stability with the observed current response diminishing with time. This limited stability has also been observed by Bryce and co-workers for similar compounds [14,16]. The importance of traces of moisture for the stability of the second redox process has been outlined by Khodorkovsky and co-workers [85]. However, the dication exhibits increased stability under argon. As such, it is probable that the instability involves reaction of $\mathbf{1}^{2+}$ and molecular oxygen, but moisture may also play a role [86–89]. As a result the spectroscopic features obtained for this species may be affected.

The electronic features of $\mathbf{1}^{2+}$ are shown in Fig. 4. Applying a potential of 1.1 V (*vs.* Ag wire) results in the formation of the dication. This is indicated in Fig. 4 (dashed line) by a further decrease in the absorbance bands at 280, 290, 316 and 346 nm. The absorbance bands at 424, 457, 479, 561 and 924 nm, observed for $\mathbf{1}^{\bullet+}$ also appear with much weaker intensity in the spectrum of $\mathbf{1}^{2+}$. There is an absence of an isosbestic point in the spectra upon reduction back to **1** indicating that full reversibility is not observed (Fig. 4). This suggests that the dication has limited stability under the conditions and timescale (~75 min) of the experiment even when under an argon atmosphere.

3.5. Surface immobilisation of *1*

Cyclic voltammetry of **1** immobilised on an electrode surface in aerated solution shows two oxidation waves (not shown). A linear relationship between the peak current, i_p, and the scan rate, ν, is observed under aerobic conditions, which is characteristic of a surface confined process. The ΔE_p values observed for a monolayer of **1** are greater than zero with the anodic and cathodic current maxima separated by a minimum of 40 mV (ν = 7 V/s) and a maximum of 90 mV (ν = 30 V/s). The FWHM, calculated for the redox waves in the CV, ranges from 120–160 mV. As the scan rate increases, ΔE_p

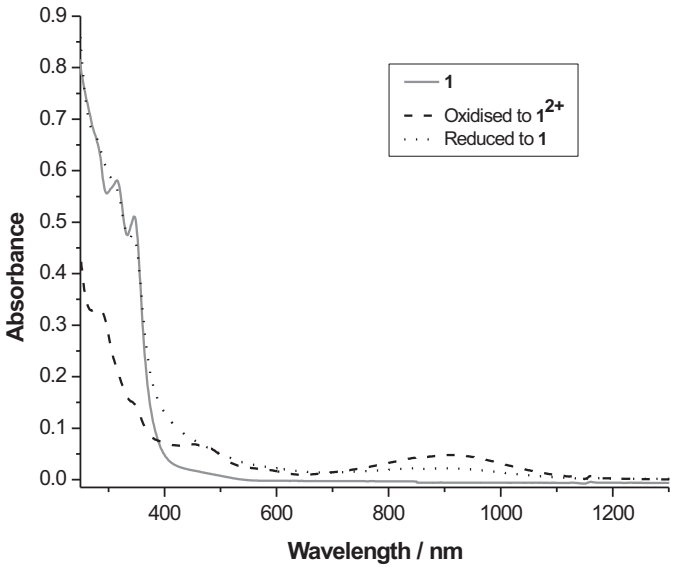

Fig. 4. Spectral variations of **1** (solid grey line) under controlled electrochemical oxidation (E = +1.1 V, *vs.* Ag wire) to $\mathbf{1}^{2+}$ (dashed black line) and reduction back to **1** (dotted black line). The spectra were recorded in CH_2Cl_2 (0.1 M $TBAPF_6$) under argon using a Pt gauze working electrode.

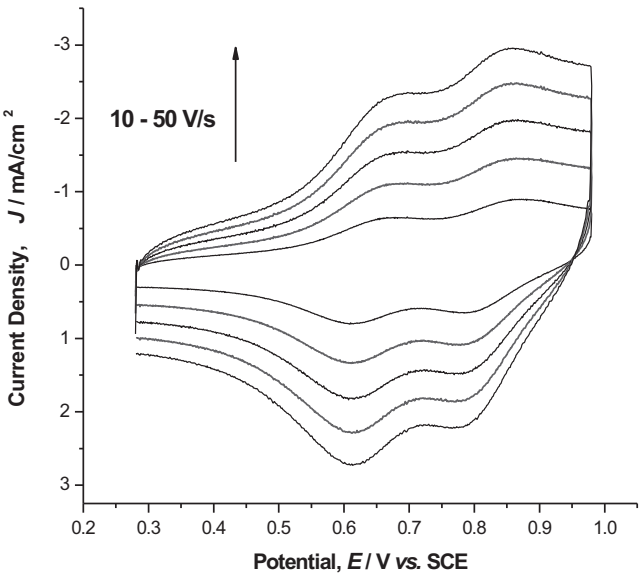

Fig. 5. Cyclic voltammetry of a monolayer of **1** on a Pt electrode (real surface area = 0.116 cm^2) following immersion in a 500 μM solution of the compound in CH_2Cl_2, using 0.1 M $TBAClO_4$ in acetonitrile. CVs were recorded under argon.

Table 4
ΔE_p and surface coverage of monolayers of **1** on a Pt electrode under aerobic and anaerobic conditions in acetonitrile (0.1 M $TBAClO_4$).

Scan rate	ΔE_p (mV) **1**–**1**$^+$	ΔE_p (mV) **1**$^+$–**1**$^{2+}$	Surface coverage, Γ (mol cm^{-2})
Aerobic conditions			
5 V/s	40 (a)	45 (a)	5×10^{-12} (a)
	35 (b)	45 (b)	3×10^{-12} (b)
Anaerobic conditions			
10 V/s	60 (a)	80 (a)	1×10^{-11} (a)
	60 (b)	80 (b)	1×10^{-11} (b)

The final scan was recorded after cycling with scan rates up to 50 V/s (approximately 5 min). a = initial scan, b = final scan.

also increases possibly suggesting that slow charge transfer kinetics are associated with the observed response [39].

The CVs of **1** under these conditions on Pt, show the surface coverage of the monolayer, is in the order of 10^{-12} mol cm^{-2} (Table 4). For a dense monolayer, a surface coverage in the range of 10^{-10} mol cm^{-2} is expected [90]. The value calculated for the monolayer analysed in air is almost two orders of magnitude lower than this optimum value which suggests that under aerobic conditions a dense monolayer is not recorded on Pt. Further analysis of the surface coverage in air, shows a decrease by approximately 40% after the potential is applied over the range of scan rates.

Oxidation of **1** to $\mathbf{1}^{2+}$ under air indicates a lack of stability of the assembly on a surface as has been reported previously [14,16,91]. However, restricting the potential to the formation of the monocation redox intermediate resulted in more stable responses.

The behaviour of the monolayers under argon is shown in Fig. 5. As shown for the monolayer in air, the ΔE_p values observed are greater than zero and the anodic and cathodic current maxima are separated by a minimum of 60 mV (ν = 10 V/s) and a maximum of 80 mV (ν = 50 V/s). The FWHM, calculated for the redox waves in the CV, ranges from 110 to 140 mV. Increasing the scan rate from 10 to 50 V/s results in minimal changes in the peak potential (E_p). A value of approximately 1×10^{-11} mol cm^{-2} was estimated for the surface coverage at the initial scan rate of 10 V/s with a projected area per molecule of 1640 $Å^2$. When the monolayer was subsequently scanned at up to 50 V/s before final scanning at 10 V/s the surface coverage had not significantly changed, even when the scan included the oxidation to the dication as shown in Fig. 5.

So $\mathbf{1}^{2+}$ is unstable in air both under solution-phase diffusion controlled conditions and when immobilised on the surface which is likely due to its exposure to oxygen in the surrounding environment. Under argon a considerable improvement of the stability of the monolayer is observed.

3.6. Modelling of electronic properties

The parent tetrathiafulvalene (TTF) and bis(ethylenedithio) tetrathiafulvalene (BEDT-TTF, **2**) were modelled by Andreu et al. [81] Their comparison of different functionals and basis sets showed that the hybrid functionals B3P86 and B3PW91 are superior over the common B3LYP for geometry optimisations. Furthermore, they pointed out that the different basis sets (6-31G(d), 6-31+G(d), 6-311+G(d,p), cc-pVDZ, aug-cc-pVDZ) used with these functionals had little influence on the results of single point TD-DFT calculations. We also found B3PW91/6-31+G(d) to give good accuracy for geometry optimisation of **1**, $\mathbf{1}^{\bullet+}$, the singlet dication $^1\mathbf{1}^{2+}$ and **2**. Application of CH_2Cl_2 as solvent for the SCRF calculations is appropriate since the Gutmann donor number is 0 (*vide supra*) and thus orbital interactions can be neglected. One should therefore be able to model the influence of this solvent by an SCRF procedure.

3.7. DFT modelling of electronic and electrochemical properties

Density functional theory was employed in order to shine light on the localisation of the frontier orbitals of **1**, $\mathbf{1}^{\bullet+}$ and $^1\mathbf{1}^{2+}$, as well as on the localisation of the low energy transitions observed by spectroelectrochemistry. In agreement with X-ray diffraction results, the compounds **1**, $\mathbf{1}^{\bullet+}$, $^1\mathbf{1}^{2+}$ and **2** were optimised in boat conformations (Fig. 6) and are in excellent agreement with experimental data [38,92]. The calculated structural changes introduced by oxidising **1** to $\mathbf{1}^{\bullet+}$ are in good agreement with the changes observed by Almeida and co-workers in the solid state

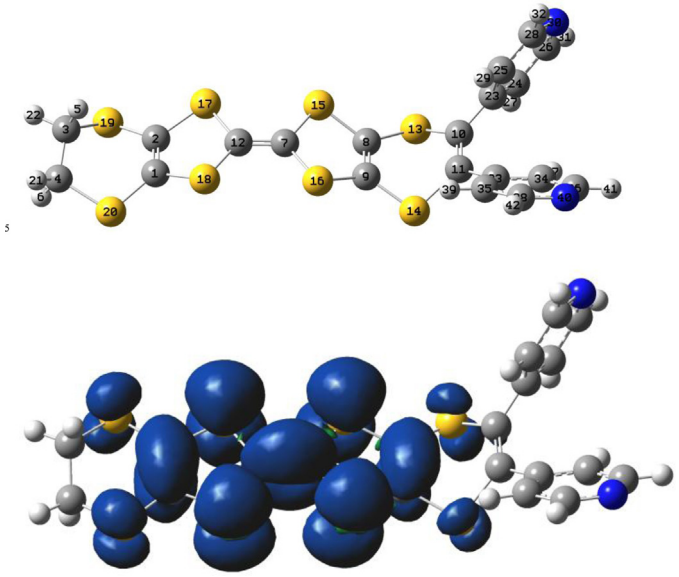

Fig. 6. Presentation of the optimised structure of **1** (above). Presentation of the calculated spin density of $\mathbf{1}^{\bullet+}$ (CPCM-B3PW91/6-31+G(d)) (below).

[38]. Furthermore, the experimental observations indicate that the unpaired electron and hence the positive charge is located on the TTF moiety, which is in agreement with the calculated spin density shown in Fig. 6.

Contributions from atoms or groups to the frontier orbitals in the ground state were investigated. The results were compared with the data obtained for **2** to examine the extent of contributions of the pendant pyridyl groups. In **1**, these substituents have no orbital contributions to the HOMO. In both compounds **1** and **2**, the HOMO is localised on the TTF moiety. The pyridyl rings mainly contribute to the LUMO of **1** as well as to lower lying occupied states. In accord with the interpretation of the electrochemical data, oxidation of **1** removes an electron from the TTF core (HOMO), while reduction furnishes a radical anion with a significant probability on the pyridyl substituents. Oxidation of **1** to $\mathbf{1}^{\bullet+}$ yields a singly occupied orbital (SOMO), which is also located on the TTF moiety (*cf.* spin density in Fig. 6) and is the location for the second oxidation from $\mathbf{1}^{\bullet+}$ to $^{1}\mathbf{1}^{2+}$ yielding a TTF core based LUMO of $^{1}\mathbf{1}^{2+}$. Although fully delocalised orbitals are found among the frontier orbitals (*e.g.* L+3 of **1**) the pyridyl substituents leave the electronic properties of EVT-TTF nearly unaffected.

Information about the nature of the near-IR transitions observed by spectroelectrochemistry was further investigated by time-dependent DFT (TD-DFT) calculations (Fig. 7). Theoretical investigations were performed with **1**, $\mathbf{1}^{\bullet+}$ and $^{1}\mathbf{1}^{2+}$ using the B3PW91, M06HF and BMK functionals with the 6-31+G(d) basis as well as on the larger BMK/def2-TZVPP+R level. The B3PW91 functional satisfactorily modelled electron excitation of the uncharged compound **1**. Satisfactory results were obtained also for the lowest energy transition of $\mathbf{1}^{\bullet+}$ and $^{1}\mathbf{1}^{2+}$, although at slightly lower energies. Modelling of the high energy transitions furnished unsatisfactory results at the B3PW91/6-31+G(d) level. They were therefore compared to BMK functional of Boese and Martin [60] as well as to the M06HF functional of Zhao and Truhlar [61]. M06HF gave unsatisfactory results for both the charged and uncharged species. The BMK functional was able to model the low energy transitions of the charged species. But the higher energy transitions could still not be satisfactorily modelled. Additionally, the large def2-TZVPP+R basis was applied where 1s1p1d diffuse Gaussian Rydberg functions are added to sulphur [62,63]. This basis turned out to be superior over TZVP and TZVPP for

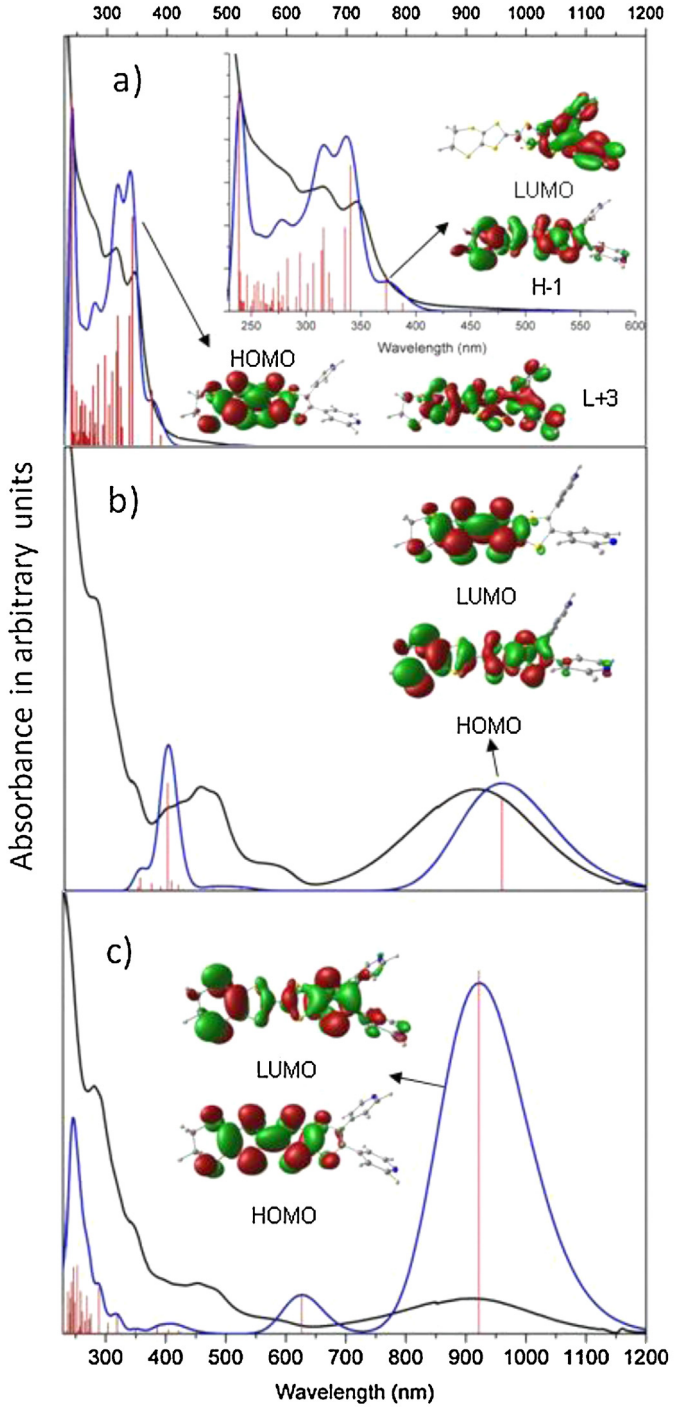

Fig. 7. Comparison of calculated (blue) and experimental (black) electron excitation features of **1** (a), $\mathbf{1}^{+}$ (b) and $^{1}\mathbf{1}^{2+}$ (c). Calculated transitions are given in red and were used to calculate the blue spectrum with a FWHM of 2000 cm^{-1}. The donor and acceptor orbitals of the lowest energy transitions are given. Calculated values were obtained by TD-DFT on the CPCM-B3PW91/6-31+G(D) (a and b) CPCM-BMK/6-31+G(D) (c) level of theory. Dichloromethane was used to model the solvent sphere. The inset in (a) depicts the spectrum between 230 and 500 nm. (For interpretation of the references to colour in this figure legend, the reader is referred to the web version of this article.)

vertical excitation energies of thiophene [62] but did not give satisfactory results for the high energy transition of $\mathbf{1}^{\bullet+}$ and $^{1}\mathbf{1}^{2+}$.

The low energy bands of the experimental spectra of **1** and **2** are similar in energy. The lowest energy band in **2** can be

assigned to a HOMO $\pi \rightarrow$ LUMO σ^* transition and is a TTF core based transition. For **1** the lowest energy transition occurs as a flat shoulder in the experimental spectrum and could only satisfactorily be modelled on the B3PW91/6-31+G(d) level. This feature is assigned to a HOMO-1 → LUMO transition with charge transfer from the TTF-core to the pyridyl substituents. The BMK/6-31+G(d) and BMK/TZVPP+R model chemistries also predict a small shoulder which is blue shifted and assigned to a HOMO → LUMO + 1 transition. In accordance with the B3PW91 results significant charge transfer to the pyridyl substituents is found. All three model chemistries predict an intensive low energy HOMO → LUMO + 3 transition but with a significant blue shift for the BMK calculations. Thereby an electron is transferred from the TTF-core to the fully delocalized LUMO + 3. The low energy near infrared absorptions of $\mathbf{1}^{\bullet+}$ and $^{1}\mathbf{1}^{2+}$ are known features of this type of cation. The employed model chemistries were only able to predict the low energy band but failed for the higher energy absorptions. Although slightly different in the predicted energies (0.01–0.14 eV), all three models predict a transition from the highest doubly occupied molecular orbital (HDOMO) to the SOMO of $\mathbf{1}^{\bullet+}$. Electron transfer occurs from an orbital delocalised on the vinylenedithio-TTF moiety of $\mathbf{1}^{\bullet+}$ to the TTF core based SOMO. The same charge transfer is predicted for the lowest energy band of $^{1}\mathbf{1}^{2+}$ representing a HOMO → LUMO transition.

4. Conclusions

In the present contribution, the redox and spectroscopic properties, together with molecular modelling of a vinylenedithio-TTF derivative, **1**, have been examined. Two redox waves are observed for **1**, the ΔE values of which are solvent dependent. Stabilisation of the monocation intermediate ($\mathbf{1}^{\bullet+}$) towards further oxidation is achieved in solvents with a low Gutmann donor number. Successful formation of a monolayer of **1** has been achieved on platinum, a less common substrate for monolayers of TTF type compounds, without the use of long alkyl chain linker groups which can be disadvantageous in the fabrication of molecular electronic devices [37]. This monolayer is stable in deaerated solvents but in the presence of oxygen the dication formed is decomposed. Normally, the presence of oxygen is not a problem when carrying out electrochemical oxidations at these potentials. In this case however, the dication formed is most likely involved in a chemical reaction which leads to its decomposition. As a result of the decomposition process the spectroelectrochemical data observed for the dication needs to be treated with care. The compound can be immobilised on Pt surfaces but surface coverage values suggest that sparse monolayers are formed. From these data alone it is not possible to determine if the monolayer is formed on Pt *via* the nitrogen atom of the pyridine ring, monolayers of which have been reported by Forster et al. [39], or whether the molecules stack parallel to the surface for example through π-stacking, as has been shown for graphene and graphite surfaces [35]. TD-DFT calculations reveal a HOMO that is predominantly located on the TTF core and that the addition of pyridine rings does not affect the attractive oxidative properties of the TTF unit. In addition, the modelling of vertical excitations with TD-DFT and the applied model chemistries gives acceptable results for the low energy transitions but is less satisfactory for high energy transitions.

Acknowledgement

The authors thank COST D35 for financial support. JW thanks EPSRC for support. YH and JGV thank Science Foundation Ireland (grant number: 06/RFP/029) for supporting this work.

References

[1] F. Wudl, D. Wobschal, E.J. Hufnagel, Electrical conductivity by the bis-1,3-dithiole-bis-1,3-dithiolium system, Journal of the American Chemical Society 94 (1972) 670.
[2] M. Bendikov, F. Wudl, D.F. Perepichka, Tetrathiafulvalenes, oligoacenenes, and their buckminsterfullerene derivatives: the brick and mortar of organic electronics, Chemical Reviews 104 (2004) 4891.
[3] P. Batail, Introduction: molecular conductors, Chemical Reviews 104 (2004) 4887.
[4] C. Rovira, Bis(ethylenethio)tetrathiafulvalene (BET-TTF) and related dissymmetrical electron donors: from the molecule to functional molecular materials and devices (OFETs), Chemical Reviews 104 (2004) 5289.
[5] J. Ferraris, D.O. Cowan, V. Walatka, J.H. Perlstein, Electron transfer in a new highly conducting donor-acceptor complex, Journal of the American Chemical Society 95 (1973) 948.
[6] M.R. Bryce, Tetrathiafulvalenes as p-electron donors for intramolecular charge-transfer materials, Advanced Materials 11 (1999) 11.
[7] Y. Geng, X.J. Wang, B. Chen, H. Xue, Y.P. Zhao, S. Lee, C.H. Tung, L.Z. Wu, Semiconducting neutral microstructures fabricated by coordinative self-assembly of intramolecular charge-transfer tetrathiafulvalene derivatives, Chemistry – A European Journal 15 (2009) 5124.
[8] Q.Y. Zhu, L.B. Huo, Y.R. Qin, Y.P. Zhang, Z.J. Lu, J.P. Wang, J. Dai, Triadic intramolecular charge transfer compound of tetrathiafulvalene exhibiting multicolor solvatochromism, Journal of Physical Chemistry B 114 (2010) 361.
[9] J. Boixel, J. Fortage, E. Blart, Y. Pellegrin, L. Hammarström, H.C. Becker, F. Odobel, Extension of the charge separated-state lifetime by supramolecular association of a tetrathiafulvalene electron donor to a zinc/gold bisporphyrin, Dalton Transactions 39 (2010) 1450.
[10] M.B. Nielsen, C. Lomholt, J. Becher, Tetrathiafulvalenes as building blocks in supramolecular chemistry II, Chemical Society Reviews 29 (2000) 153.
[11] T. Jørgensen, T.K. Hansen, J. Becher, Tetrathiafulvalenes as building-blocks in supramolecular chemistry, Chemical Society Reviews 23 (1994) 41.
[12] N. Martín, J.-L. Segura, New concepts in tetrathiafulvalene chemistry, Angewandte Chemie International Edition 40 (2001) 1372.
[13] J. Lyskawa, M. Oçafrain, G. Trippé, F. Le Derf, M. Sallé, P. Viel, S. Palacin, Tetrathiafulvalene-based podands bearing one or two thiol functions: immobilization as self-assembled monolayers or polymer films and recognition properties, Tetrahedron 62 (2006) 4419.
[14] A.J. Moore, L.M. Goldenberg, M.R. Bryce, M.C. Petty, A.P. Monkman, C. Marenco, J. Yarwood, M.J. Joyce, S.N. Port, Cation recognition by self-assembled layers of novel crown-annelated tetrathiafulvalenes, Advanced Materials 10 (1998) 395.
[15] H. Liu, S. Liu, L. Echegoyen, Remarkably stable self-assembled monolayers of new crown-ether annelated tetrathiafulvalene derivatives and their cation recognition properties, Chemical Communications (1999) 1493.
[16] A.J. Moore, L.M. Goldenberg, M.R. Bryce, M.C. Petty, J. Moloney, J.A.K. Howard, M.J. Joyce, S.N. Port, New crown annelated tetrathiafulvalenes: synthesis, electrochemistry, self-assembly of thiol derivatives, and metal cation recognition, Journal of Organic Chemistry 65 (2000) 8269.
[17] H. Kim, W.A. Goddard III, S.S. Jang, W.R. Dichtel, J.R. Heath, J.F. Stoddart, Free energy barrier for molecular motions in bistable [2]rotaxane molecular electronic devices, Journal of Physical Chemistry A 113 (2009) 2136.
[18] E. Leary, S.J. Higgins, H. van Zalinge, W. Haiss, R.J. Nichols, S. Nygaard, J.O. Jeppesen, J. Ulstrup, Structure-property relationships in redox-gated single molecule junctions – a comparison of pyrrolo-tetrathiafulvalene and viologen redox groups, Journal of the American Chemical Society 130 (2008) 12204.
[19] F. Giacalone, M.A. Herranz, L. Grüter, M.T. González, M. Calame, C. Schönenberger, C.R. Arroyo, G. Rubio-Bollinger, M. Vélez, N. Agraït, N. Martín, Tetrathiafulvalene-based molecular nanowires, Chemical Communications (2007) 4854.
[20] E. Gomar-Nadal, G.K. Ramachandran, F. Chen, T. Burgin, C. Rovira, D.B. Amabilino, S.M. Lindsay, Self-assembled monolayers of tetrathiafulvalene derivatives on Au(1 1 1): organization and electrical properties, Journal of Physical Chemistry B 108 (2004) 7213.
[21] D. Canevet, M. Sallé, G. Zhang, D. Zhang, D. Zhu, Tetrathiafulvalene (TTF) derivatives: key building-blocks for switchable processes, Chemical Communications (2009) 2245.
[22] M. Mas-Torrent, C. Rovira, Novel small molecules for organic field-effect transistors: towards processability and high performance, Chemical Society Reviews 37 (2008) 613.
[23] G. Yzambart, B. Fabre, F. Camerel, T. Roisnel, D. Lorcy, Controlled grafting of tetrathiafulvalene (TTF) containing diacetylenic units on hydrogen-terminated silicon surfaces: from redox-active TTF monolayer to polymer films, Journal of Physical Chemistry C 116 (2012) 12093.
[24] G. Ho, J.R. Heath, M. Kondratenko, D.F. Perepichka, K. Arseneault, M. Pezolet, M.R. Bryce, The first studies of a tetrathiafulvalene-s-acceptor molecular rectifier, Chemistry – A European Journal 11 (2005) 2914.
[25] A. Aviram, M.A. Ratner, Molecular rectifiers, Chemical Physics Letters 29 (1974) 277.
[26] E. Gomar-Nadal, J. Puigmartí-Luis, D.B. Amabilino, Assembly of functional molecular nanostructures on surfaces, Chemical Society Reviews 37 (2008) 490.
[27] H. Fujihara, H. Nakai, M. Yoshihara, T. Maeshima, Alkane-tetrathiol induced formation of remarkably stable self-assembled monolayer and polymer films containing electroactive tetrathiafulvalene moieties on metal electrodes, Chemical Communications (1999) 737.

[28] C.M. Yip, M.D. Ward, Self-assembled monolayers with charge-transfer groups: n-mercaptoalkyl tetrathiafulvalene carboxylate on gold, Langmuir 10 (1994) 549.
[29] G. Trippé, M. Ocafrain, M. Besbes, V. Monroche, J. Lyskawa, F. Le Derf, M. Sallé, J. Becher, B. Colonna, L. Echegoyen, Self-assembled monolayers of a tetrathiafulvalene-based redox-switchable ligand, New Journal of Chemistry 26 (2002) 1320.
[30] P.-Y. Blanchard, O. Alévêque, S. Boisard, C. Gautier, A. El-Ghayoury, F. Le Derf, T. Breton, E. Levaillain, Intermolecular interactions in self-assembled monolayers of tetrathiafulvalene derivatives, Physical Chemistry Chemical Physics 13 (2011) 2118.
[31] S.-G. Liu, H. Liu, K. Bandyopadhyay, Z. Gao, L. Echegoyen, Dithia-crown-annelated tetrathiafulvalene disulfides: synthesis, electrochemistry, self-assembled films, and metal ion recognition, Journal of Organic Chemistry 65 (2000) 3292.
[32] H.-R. Tseng, D. Wu, N.X. Fang, X. Zhang, J.F. Stoddart, The metastability of an electrochemically controlled nanoscale machine on gold surfaces, ChemPhysChem 5 (2004) 111.
[33] W.F. Paxton, S.L. Kleinman, A.N. Basuray, J.F. Stoddart, R.P. Van Duyne, Surface-enhanced Raman spectroelectrochemistry of TTF-modified self-assembled monolayers, The Journal of Physical Chemistry Letters 2 (2011) 1145.
[34] G. Yzambart, B. Fabre, D. Lorcy, Multiredox tetrathiafulvalene-modified oxide-free hydrogen-terminated Si(1 0 0) surfaces, Langmuir 28 (2012) 3453.
[35] J. Puigmartí-Luis, A. Minoia, H. Uji-i, C. Rovira, J. Cornil, S. De Feyter, R. Lazzaroni, D.B. Amabilino, Noncovalent control for bottom-up assembly of functional supramolecular wires, Journal of the American Chemical Society 128 (2006) 12602.
[36] M.M.S. Abdel-Mottaleb, E. Gomar-Nadal, M. Surin, H. Uji-i, W. Mamdouh, J. Veciana, V. Lemaur, C. Rovira, J. Cornil, R. Lazzaroni, D.B. Amabilino, S. De Feyter, F.C. De Schryver, Self-assembly of tetrathiafulvalene derivatives at a liquid/solid interface—compositional and constitutional influence on supramolecular ordering, Journal of Materials Chemistry 15 (2005) 4601.
[37] R. Yuge, A. Miyazaki, T. Enoki, K. Tamada, F. Nakamura, M. Hara, Fabrication of TTF–TCNQ charge-transfer complex self-assembled monolayers: comparison between the coadsorption method and the layer-by-layer adsorption method, Journal of Physical Chemistry B 106 (2002) 6894.
[38] A.C. Brooks, P. Day, S.I.G. Dias, S. Rabaça, I.C. Santos, R.T. Henriques, J.D. Wallis, M. Almeida, Pyridine-functionalised (vinylenedithio)tetrathiafulvalene (VDT–TTF) derivatives and their dithiolene analogues, European Journal of Inorganic Chemistry (2009) 3084.
[39] R.J. Forster, L.R. Faulkner, Electrochemistry of spontaneously adsorbed monolayers. Equilibrium properties and fundamental electron transfer characteristics, Journal of the American Chemical Society 116 (1994) 5444.
[40] R.J. Forster, L.R. Faulkner, Electrochemistry of spontaneously adsorbed monolayers. Effects of solvent, potential, and temperature on electron transfer dynamics, Journal of the American Chemical Society 116 (1994) 5453.
[41] R.J. Forster, E. Figgemeier, A. Lees, J. Hjelm, J.G. Vos, Photostability, electrochemistry and monolayers of [M(bpy)2(trans-1,2-bis(4-pyridyl) ethylene)L] + (M = Ru, Os, L = Cl, H_2O), Langmuir 16 (2000) 7867.
[42] T. Albrecht, K. Moth-Poulsen, J.B. Christensen, A. Guckian, T. Bjørnholm, J.G. Vos, J. Ulstrup, In situ scanning tunnelling spectroscopy of inorganic transition metal complexes, Faraday Discussions 131 (2006) 265.
[43] T. Albrecht, A. Guckian, A.M. Kuznetsov, J.G. Vos, J. Ulstrup, Mechanism of electrochemical charge transport in individual transition metal complexes, Journal of the American Chemical Society 128 (2006) 17132.
[44] T. Albrecht, A. Guckian, J. Ulstrup, J.G. Vos, Transistor effects and in situ STM of redox molecules at room temperature, IEEE Transactions on Nanotechnology 4 (2005) 430.
[45] T. Albrecht, A. Guckian, J. Ulstrup, J.G. Vos, Transistor-like behavior of transition metal complexes, Nano Letters 5 (2005) 1451.
[46] H. Nakano, K. Miyawaki, T. Nogami, Y. Shirota, S. Harada, N. Kasai, The synthesis of 4,5-ethylenedithio-4′,5′-vinylenedithiotetrathiafulvalene (EVT) and its methyl and dimethyl derivatives (EMVT, EDMVT), and the molecular and crystal-structures of EVT, Bulletin of the Chemical Society of Japan 62 (1989) 2604.
[47] M.J. Frisch, G.W. Trucks, H.B. Schlegel, G.E. Scuseria, M.A. Robb, J.R. Cheeseman, J.J.A. Montgomery, T. Vreven, K.N. Kudin, J.C. Burant, J.M. Millam, S.S. Iyengar, J. Tomasi, V. Barone, B. Mennucci, M. Cossi, G. Scalmani, N. Rega, G.A. Petersson, H. Nakatsuji, M. Hada, M. Ehara, K. Toyota, R. Fukuda, J. Hasegawa, M. Ishida, T. Nakajima, Y. Honda, O. Kitao, H. Nakai, M. Klene, X. Li, J.E. Knox, H.P. Hratchian, J.B. Cross, V. Bakken, C. Adamo, J. Jaramillo, R. Gomperts, R.E. Stratmann, O. Yazyev, A.J. Austin, R. Cammi, C. Pomelli, J.W. Ochterski, P.Y. Ayala, K. Morokuma, G.A. Voth, P. Salvador, J.J. Dannenberg, V.G. Zakrzewski, S. Dapprich, A.D. Daniels, M.C. Strain, O. Farkas, D.K. Malick, A.D. Rabuck, K. Raghavachari, J.B. Foresman, J.V. Ortiz, Q. Cui, A.G. Baboul, S. Clifford, J. Cioslowski, B.B. Stefanov, G. Liu, A. Liashenko, P. Piskorz, I. Komaromi, R.L. Martin, D.J. Fox, T. Keith, M.A. Al-Laham, C.Y. Peng, A. Nanayakkara, M. Challacombe, P.M.W. Gill, B. Johnson, W. Chen, M.W. Wong, C. Gonzalez, J.A. Pople, Gaussian 03, Revision D. 01, 2004.
[48] A.D. Becke, Density functional thermochemistry. III. The role of exact exchange, Journal of Chemical Physics 98 (1993) 5648.
[49] J.P. Perdew, Density-functional approximation for the correlation energy of the inhomogeneous electron gas, Physical Review B 33 (1986) 8822.
[50] J.P. Perdew, K. Burke, Y. Wang, Generalized gradient approximation for the exchange-correlation hole of a many-electron system, Physical Review B 54 (1996) 16533.
[51] J.P. Perdew, J.A. Chevary, S.H. Vosko, K.A. Jackson, M.R. Pederson, D.J. Singh, C. Fiolhais, Erratum: atoms, molecules, solids, and surfaces: applications of the generalized gradient approximation for exchange and correlation, Physical Review B 48 (1993) 4978.
[52] J.P. Perdew, J.A. Chevary, S.H. Vosko, K.A. Jackson, M.R. Pederson, D.J. Singh, C. Fiolhais, Atoms, molecules, solids, and surfaces: applications of the generalized gradient approximation for exchange and correlation, Physical Review B 46 (1992) 6671.
[53] P. Csaszar, P.J. Pulay, Geometry optimization by direct inversion in the iterative subspace, Journal of Molecular Structure 114 (1984) 31.
[54] O. Farkas, Ph.D. Thesis, Eötvös Loránd University and Hungarian Academy of Sciences, Budapest, 1995.
[55] O. Farkas, H.B. Schlegel, Methods for optimizing large molecules. II. Quadratic search, Journal of Chemical Physics 111 (1999) 10806.
[56] R. Bauernschmitt, R. Ahlrichs, Treatment of electronic excitations within the adiabatic approximation of time dependent density functional theory, Chemical Physics Letters 256 (1996) 454.
[57] M.E. Casida, C. Jamorski, K.C. Casida, D.R. Salahub, Molecular excitation energies to high-lying bound states from time-dependent density-functional response theory: characterization and correction of the time-dependent local density approximation ionization threshold, Journal of Chemical Physics 108 (1998) 4439.
[58] R.E. Stratmann, G.E. Scuseria, M.J. Frisch, An efficient implementation of time-dependent density-functional theory for the calculation of excitation energies of large molecules, Journal of Chemical Physics 109 (1998) 8218.
[59] M.J. Frisch, G.W. Trucks, H.B. Schlegel, G.E. Scuseria, M.A. Robb, J.R. Cheeseman, G. Scalmani, V. Barone, B. Mennucci, G.A. Petersson, H. Nakatsuji, M. Caricato, X. Li, H.P. Hratchian, A.F. Izmaylov, J. Bloino, G. Zheng, J.L. Sonnenberg, M. Hada, M. Ehara, K. Toyota, R. Fukuda, J. Hasegawa, M. Ishida, T. Nakajima, Y. Honda, O. Kitao, H. Nakai, T.J.A. Vreven, J. Montgomery, J.E. Peralta, F. Ogliaro, M. Bearpark, J.J. Heyd, E. Brothers, K.N. Kudin, V.N. Staroverov, R. Kobayashi, J. Normand, K. Raghavachari, A. Rendell, J.C. Burant, S.S. Iyengar, J. Tomasi, M. Cossi, N. Rega, J.M. Millam, M. Klene, J.E. Knox, J.B. Cross, V. Bakken, C. Adamo, J. Jaramillo, R. Gomperts, R.E. Stratmann, O. Yazyev, A.J. Austin, R. Cammi, C. Pomelli, J.W. Ochterski, R.L. Martin, K. Morokuma, V.G. Zakrzewski, G.A. Voth, P. Salvador, J.J. Dannenberg, S. Dapprich, A.D. Daniels, O. Farkas, J.B. Foresman, J.V. Ortiz, J. Cioslowski, D.J. Fox, Gaussian 09, Revision A. 02, 2009.
[60] A.D. Boese, J.M.L. Martin, Development of density functionals for thermochemical kinetics, Journal of Chemical Physics 121 (2004) 3405.
[61] Y. Zhao, D.G. Truhlar, The M06 suite of density functionals for main group thermochemistry, thermochemical kinetics, noncovalent interactions, excited states, and transition elements: two new functionals and systematic testing of four M06-class functionals and 12 other functionals, Theoretical Chemistry Accounts 120 (2008) 215.
[62] S. Salzmann, M. Kleinschmidt, J. Tatchen, R. Weinkauf, C.M. Marian, Excited states of thiophene: ring opening as deactivation mechanism, Physical Chemistry Chemical Physics 10 (2008) 380.
[63] Molcas online tutorial, Lund University, http://www.teokem.lu.se/molcas/tutor, 2002.
[64] V. Barone, M. Cossi, Quantum calculation of molecular energies and energy gradients in solution by a conductor solvent model, Journal of Physical Chemistry A 102 (1998) 1995.
[65] M. Cossi, N. Rega, G. Scalmani, V. Barone, Energies, structures, and electronic properties of molecules in solution with the C-PCM solvation model, Journal of Computers and Chemistry 24 (2003) 669.
[66] D. Jacquemin, E.A. Perpete, I. Ciofini, C. Adamo, Assessment of functionals for TD–DFT calculations of singlet–triplet transitions, Journal of Chemical Theory and Computation 6 (2010) 1532.
[67] N.M. O'Boyle, A.L.K.M. Tenderholt, Langner, cclib: a library for package-independent computational chemistry algorithms, Journal of Computers and Chemistry 29 (2008) 839.
[68] K. Hervé, S. Liu, O. Cador, S. Golhen, Y. Le Gal, A. Bousseksou, H. Stoeckli-Evans, S. Decurtins, L. Ouahab, Synthesis of a BEDT-TTF bipyridine organic donor and the first FeII coordination complex with a redox-active ligand, European Journal of Inorganic Chemistry (2006) 3498.
[69] M.R. Bryce, G.J. Marshallsay, A.J. Moore, Bis- and tris(tetrathiafulva1enes) (TTFs) derived from reactions of the TTF-thiolate anion, Journal of Organic Chemistry 57 (1992) 4859.
[70] C. Jia, D. Zhang, Y. Xu, W. Xu, H. Hu, D. Zhu, New TTF derivatives with pyridine groups: synthesis, electrochemical studies, crystal structure and formation of conducting LB films, Synthetic Metals 132 (2003) 249.
[71] H. Qiu, C. Wang, J. Xu, G. Lai, Y. Shen, Synthesis, spectroscopic, and electrochemical properties of three tetrathiafulvalenes attached to perylene, Monatshefte für Chemie 139 (2008) 1357.
[72] M. González, B. Illescas, N. Martín, J.L. Segura, C. Seoane, M. Hanack, Synthesis and electrochemistry of soluble double-bridged tetrathiafulvalene (TTF)-p-benzoquinone dyads, Tetrahedron 54 (1998) 2853.
[73] A. Cisak, P.J. Elving, Electrochemistry in pyridine IV. Chemical and electrochemical reduction of pyridine, Electrochimica Acta 10 (1965) 935.
[74] V. Gutmann, The Donor–Acceptor Approach to Molecular Interactions, Plenum, New York, 1978.
[75] D.A. Skoog, F.J. Holler, T.A. Nieman, Principles of Instrumental Analysis, 5th ed., Harcourt Brace & Company, Florida, 1998.
[76] D.R. Lide, Handbook of Organic Solvents, CRC Press, Florida, 1995.
[77] D.T. Sawyer, A. Sobkowiak, J.L. Roberts Jr., Electrochemistry for Chemists, 2nd ed., John Wiley, Sons, USA, 1995.

[78] W.R. Browne, J.J.D. de Jong, T. Kudernac, M. Walko, L.N. Lucas, K. Uchida, J.H. van Esch, B.L. Feringa, Oxidative electrochemical switching in dithienylcyclopentenes, part 1: effect of electronic perturbation on the efficiency and direction of molecular switching, Chemistry – A European Journal 11 (2005) 6414.
[79] D.M. D'Alessandro, F.R. Keene, A cautionary warning on the use of electrochemical measurements to calculate comproportionation constants for mixed-valence compounds, Dalton Transactions (2004) 3950.
[80] B.D. Yeomans, L.S. Kelso, P.A. Tregloan, F.R. Keene, Redox characteristics and anion association behaviour of stereoisomeric forms of mono- and oligonuclear metal complexes using high pressure electrochemistry, European Journal of Inorganic Chemistry (2001) 239.
[81] R. Andreu, J. Garín, J. Orduna, Electronic absorption spectra of closed and open-shell tetrathiafulvalenes: the first time-dependent density-functional study, Tetrahedron 57 (2001) 7883.
[82] D.L. Coffen, J.Q. Chambers, D.R. Williams, P.E. Garrett, N.D. Canfield, Tetrathioethylenes, Journal of the American Chemical Society 93 (1971) 2258.
[83] S. Hünig, G. Kiesslich, H. Quast, D. Scheutzow, Über zweistufige redoxsysteme, X1) tetrathio-äthylene und ihre höheren oxidationsstufen, Liebigs Annalen der Chemie (1973) 310.
[84] G. Schukat, E. Fanghänel, Tetrathiafulvalene. XXII [1] redox- und spektroskopische eigenschaften von tetrathiafulvalenen (TTF) und tetraselenafulvalenen (TSF) sowie deren mono- und dikationen, Journal für Praktische Chemie 327 (1985) 767.
[85] M. Giffard, G. Mabon, E. Leclair, N. Mercier, M. Allain, A. Gorgues, P. Molinié, O. Neilands, P. Krief, V. Khodorkovsky, Oxidation of TTF derivatives using (diacetoxyiodo)benzene: a general chemical route toward cation radicals, dications, and nonstoichiometric salts, Journal of the American Chemical Society 123 (2001) 3852.
[86] W.J. Bailey, E.W. Cummins, Cyclic dienes. III. The synthesis of thiophene 1-dioxide, Journal of the American Chemical Society 76 (1954) 1932.
[87] C. Schöneich, A. Aced, K.D. Asmus, Mechanism of oxidation of aliphatic thioethers to sulfoxides by hydroxyl radicals. The importance of molecular oxygen, Journal of the American Chemical Society 115 (1993) 11376.
[88] B.L. Miller, T.D. Williams, C. Schöneich, Mechanism of sulfoxide formation through reaction of sulfur radical cation complexes with superoxide or hydroxide ion in oxygenated aqueous solution, Journal of the American Chemical Society 118 (1996) 11014.
[89] C. Arbizzani, M. Mastragostino, F. Soavi, Polythiophene S,S dioxides: an investigation on electrochemical doping, Electrochimica Acta 45 (2000) 2273.
[90] R.J. Forster, T.E. Keyes, J.G. Vos, Interfacial Supramolecular Assemblies, John Wiley & Sons Ltd., Chichester, 2003.
[91] K.-N. Kuo, P.R. Moses, J.R. Lenhard, D.C. Green, R.W. Murray, Immobilization, electrochemistry, and surface interactions of tetrathiafulvalene on chemically modified ruthenium and platinum oxide electrodes, Analytical Chemistry 51 (1979) 745.
[92] P. Guionneau, D. Chasseau, J. Howard, P. Day, Neutral bis(ethylenedithio) tetrathiafulvalene at 100 K, Acta Crystallographica Section C 56 (2000) 453.